Blimp-1 Mediates Tracheal Lumen Maturation in *Drosophila melanogaster*

Arzu Öztürk-Çolak,*,†,1 Camille Stephan-Otto Attolini,† Jordi Casanova,*,†,2 and Sofia J. Araújo*,†,‡,2

*Institut de Biologia Molecular de Barcelona (IBMB-CSIC), Parc Cientific de Barcelona, C. Baldiri Reixac 10, 08028 Barcelona, Spain, †Institut de Recerca Biomedica de Barcelona (IRB Barcelona), The Barcelona Institute of Science and Technology, C. Baldiri Reixac 10, 08028 Barcelona, Spain, and ‡Department of Genetics, Microbiology and Statistics, Faculty of Biology, University of Barcelona, 08028 Barcelona, Spain and Institute of Biomedicine University of Barcelona (IBUB)

ORCID IDs: 0000-0001-8045-320X (C.S.-O.A.); 0000-0002-4749-8913 (S.J.A.)

ABSTRACT The specification of tissue identity during embryonic development requires precise spatio-temporal coordination of gene expression. Many transcription factors required for the development of organs have been identified and their expression patterns are known; however, the mechanisms through which they coordinate gene expression in time remain poorly understood. Here, we show that hormone-induced transcription factor Blimp-1 participates in the temporal coordination of tubulogenesis in *Drosophila melanogaster* by regulating the expression of many genes involved in tube maturation. In particular, we demonstrate that Blimp-1 regulates the expression of genes involved in chitin deposition and F-actin organization. We show that Blimp-1 is involved in the temporal control of lumen maturation by regulating the beginning of chitin deposition. We also report that Blimp-1 represses a variety of genes involved in tracheal maturation. Finally, we reveal that the kinase Btk29A serves as a link between Blimp-1 transcriptional repression and apical extracellular matrix organization.

KEYWORDS Blimp-1; *Drosophila*; trachea; chitin; Btk29A; aECM

SPECIALIZED cellular functions and cell lineage fates are usually regulated by only a few key instructive transcription factors required to activate or repress specific patterns of gene expression. During the development of multicellular organisms, these events must be precisely timed. As a result, organogenesis requires an accurate spatio-temporal regulation of gene expression over extended periods. While many transcription factors required for the development of organs have been identified and their expression pinpointed spatially, the mechanisms through which they coordinate downstream gene expression in time remain poorly understood. Here, we addressed part of this question during the development of the *Drosophila melanogaster* tracheal system—a model used to study epithelial organ development. The tracheal system of *D. melanogaster* is formed by a network of epithelial tubes that requires tight temporal regulation of gene expression. Tracheal tube maturation involves the timely and spatially regulated deposition of a chitinous apical extracellular matrix (aECM), a process governed by downstream effectors of the midembryonic ecdysone hormone pulse (Chavoshi *et al.* 2010). One of these ecdysone response genes is the *D. melanogaster B-lymphocyte inducing maturation protein-1* (*Blimp-1*) (Ng *et al.* 2006; Chavoshi *et al.* 2010). *Blimp-1* is the homolog of human *Prdm1* (*positive regulatory domain containing 1*) (Huang 1994). Blimp-1/PRDM1 is a zinc finger transcriptional repressor that belongs to the Prdm gene family, and it was originally identified as a silencer of *β-interferon* gene expression (Keller and Maniatis 1991). Prdm family members contain a conserved N-terminal domain, known as a positive regulatory (PR) domain. This domain has been associated with the SET methyltransferase domain, which is important for the regulation of chromatin-mediated gene expression (Hohenauer and Moore 2012). In addition, Prdm family proteins contain multiple zinc fingers that mediate sequence-specific DNA binding and protein–protein interactions (Turner *et al.* 1994). Prdm family members modulate key cellular processes, including cell fate, and the aberrant

doi: https://doi.org/10.1534/genetics.118.301444
Manuscript received July 3, 2018; accepted for publication August 1, 2018; published Early Online June 8, 2018.
Supplemental material available at Figshare: https://doi.org/10.25386/genetics.6736427.
[1]Present address: Department of Neuroscience, The Farber Institute for Neurosciences, Kimmel Cancer Center, Thomas Jefferson University, Philadelphia, PA 19107.
[2]Corresponding authors: Institut de Biologia Molecular de Barcelona (IBMB-CSIC), The Barcelona Institute of Science and Technology, School of Biology, 08028 Barcelona, Spain. E-mail: sofiajaraujo@ub.edu; and jcrbmc@ibmb.csic.es

function of some members may lead to malignant transformation (Fog *et al.* 2012). During embryonic development, Blimp-1 controls a plethora of cell-fate decisions in many organisms (Bikoff *et al.* 2009; Hohenauer and Moore 2012). In *D. melanogaster*, *Blimp-1* serves as an ecdysone-inducible gene that regulates *ftz-f1* in pupal stages (Agawa *et al.* 2007). By acting as a transcriptional repressor, *Blimp-1* prevents the premature expression of *ftz-f1*, thereby influencing the temporal regulation of events that are crucial for insect development. The expression level and stability of Blimp-1 is critical for the precise timing of pupariation (Akagi *et al.* 2016).

Blimp-1 exerts a function in tracheal system morphogenesis during embryonic development (Ng *et al.* 2006; Öztürk-Çolak *et al.* 2016). However, the question remains as to how this transcription factor regulates tube maturation events downstream of the hormone ecdysone. Here, we studied the role of Blimp-1 in the transcriptional regulation of the regulation of tracheal tube maturation in *D. melanogaster*. We found that Blimp-1 is a transcriptional repressor of many genes involved in tracheal development and that its levels are critical for the precise timing of luminal maturation and the final stages of tubulogenesis in the embryo. Our results indicate that Blimp-1, working downstream of ecdysone, acts as a link of hormone action during tube maturation in organogenesis.

Materials and Methods

D. melanogaster strains and genetics

All *D. melanogaster* strains were raised at 25° under standard conditions. Mutant chromosomes were balanced over LacZ or GFP-labeled balancer chromosomes. Overexpression and rescue experiments were carried out either with *btl-GAL4* (kindly provided by M. Affolter) or *AbdB-GAL4* (kindly provided by E. Sánchez-Herrero) drivers at 25 or 29°. y^1w^{118} (used as wild type), $Blimp\text{-}1^{KG09531}$, and *UAS-srcGFP* are described in FlyBase; UAS-Blimp-1 (Öztürk-Çolak *et al.* 2016); $Btk29A^{k00206}$ and UAS-Btk29A (kindly provided by M. Strigini).

Embryo staging and synchronization

Embryos were staged following Campos-Ortega and Hartenstein (1985). To study temporal chitin deposition, cages were set at 25° for 2 hr, and embryos were then allowed to develop for 18, 20, 22 or 24 hr at 18° in order to obtain early and late stages 12, and early and late 13, respectively. *Blimp-1* mutant embryos were compared to *Blimp-1* heterozygotes after staining with CBP and 2A12. Heterozygote embryos were differentiated from homozygous mutant embryos by the presence or absence of a β-Gal-expressing balancer.

Synthesis of pri/tal RNA probes for in situ hybridization

The *pri/tal* RNA probes were synthesized using a PCR-based technique. The *pri* gene region [524 bp, covering all coding open reading frames (ORFs) of the gene] was defined, and the forward (5′TAATACGACTCACTATAGGTTTTTGGTCAATAC ACGGCA3′) and reverse (5′AATTAACCCTCACTAAAGGAGTT TGTGGATAAGGCACGG3′) primers were designed accordingly so that the PCR product carried the two RNA promoters T3 and T7. The gene region of interest, flanked by the T3 and T7 sequences, was amplified from previously isolated genomic DNA via PCR under standard PCR conditions. The newly synthesized RNA was then purified by precipitation, resuspended in hybridization buffer, and stored at −20°.

Immunohistochemistry, image acquisition, and processing

Standard protocols for immunostaining were applied. The following antibodies were used: rat anti-DE-cad (DCAD2, DSHB); rabbit anti-GFP (Molecular Probes); anti-Gasp mAb2A12 (DSHB); guinea pig anti-Blimp-1(S. Roy); anti-expansion and anti-rebuf (from M. Llimargas); anti-knk (from A. Uv) anti Btk29A (from M. Strigini); anti aPKC (Santa Cruz Biotechnology); and chicken anti-β-gal (Cappel). Biotinylated or Cy3-, Cy2-and Cy5-conjugated secondary antibodies (Jackson ImmunoResearch) were used at 1:300. Chitin was visualized with Fluostain (Sigma) at 1 μg/ml or CBP (Chitin Binding Probe, our own, made according to NEB protocols). Confocal images of fixed embryos were obtained either with a Leica TCS-SPE, a Leica TCS-SP2, or a Leica TCS-SP5 system. Images were processed using Fiji and assembled using Photoshop. 3D cell shape reconstructions were done using Imaris software. Quantifications of apical cell surface areas were done using Fiji (Schindelin 2012).

Fluorescent in situ hybridization

Freshly fixed embryos were washed and kept at 56° in hybridization buffer for 3 hr for prehybridization. In the last 10 min of prehybridization, probes (1:100 in hybridization Buffer) were prepared for hybridization. The probes were hybridized with the embryos at 56° overnight. The next day the embryos were washed and incubated in POD-conjugated anti-DIG (in PBT) for 1 hr. The fluorescent signal was developed by the addition of Cy3 Amplification Reagent (1:100) diluted in TSA amplification diluent and incubation at room temperature in the dark for 10 min. Finally, the embryos were either mounted in Fluoromount medium or subjected to antibody staining.

In silico analysis of Blimp-1 binding sites

The Blimp-1 position weight matrix was taken from the reported binding sequences in Kuo and Calame (2004). We extracted sequences 2000 bp upstream and downstream from all annotated isoforms in the *D. melanogaster* genome using the ENSEMBL (Cunningham *et al.* 2015) and biomaRt (Smedley *et al.* 2015) databases. All computations were performed within the R statistical framework (http://www.R-project.org). The Matscan software (Blanco *et al.* 2006) was used to find putative binding sites for the Blimp-1 position weight matrix in the aforementioned regions. For each binding site, we computed the mean conservation score of the corresponding positions following the *D. melanogaster* related species' conservation track of the UCSC browser

(Fujita *et al.* 2011). For genes with multiple transcription start sites (TSSs), nonredundant binding candidates for all TSSs were reported. Each gene was assigned with the maximum Matscan score of the corresponding binding sites after filtering by conservation score. Fisher tests were performed to find enrichment of tracheal genes among genes with predicted binding sites. All isoforms were included in the computation in order to consider multiple bindings for the same gene as this may increase the probability of binding and therefore tighter regulation.

Data availability

Fly strains are available upon request. Supplemental files contain the complete lists of possible genes/isoforms regulated by Blimp-1 and full information on the possible binding sites (Supplemental Material, Tables S1–S3), a supplemental file with all information on the files, and Figures S1 and S2. Supplemental material available at Figshare: https://doi.org/10.25386/genetics.6736427.

Results

Blimp-1 modulates tracheal tube size and apical ECM formation

Blimp-1, an ecdysone response gene (Beckstead *et al.* 2005; Chavoshi *et al.* 2010) (Figure S1), encodes the *D. melanogaster* homolog of the transcriptional factor *B-lymphocyte-inducing maturation protein* gene, whose mutants have been reported to have misshapen trachea with severe defects in taenidia (Ng *et al.* 2006; Öztürk-Çolak *et al.* 2016). Detailed expression analysis of Blimp-1 protein in tracheal cells showed that expression is not detectable until embryonic stage 12 and is then observed until stage 15 (Figure 1, A–D). At this stage, Blimp-1 protein levels started decreasing, first in dorsal trunk (DT) cells, and by stage 16 the protein was no longer detectable in any tracheal cell. In addition to its tracheal expression, Blimp-1 was also detected in the epidermal, midgut, and hindgut cells throughout these stages (Figure 1, A–D). In *Blimp-1* mutant stage 16 embryos, we detected lower levels of chitin, inflated tracheal tubes, and disorganized taenidial ridges (Öztürk-Çolak *et al.* 2016) (Figure 1, E–H).

The tube shape of *Blimp-1* mutant embryos was altered, DTs showing a smaller diameter at the fusion points than in the rest of the tubes (Figure 1H). To better study whether this phenotype was due to constrictions at fusion points and/or dilations along the entire length of the tubes, we measured the tube diameter at fusion points of tracheal metameres Tr7-Tr8 and Tr8-Tr9 and the largest tube diameter at the Tr8 metamere between fusion points. *Blimp-1* mutant embryos had a significantly (P-value: 4.4E−07, by Student's t-test, $n = 10$) larger tube diameter between fusion points than wild-type (*wt*) DTs ($n = 15$), while, at the fusion points, the tube diameter was similar to the *wt* (Figure 1I). These results suggest that *Blimp*-1 is required to maintain the luminal structures from overexpanding in between fusion points. Since tube expansion is related to the apical cell surface, we next examined cell shape and apical area in the trachea of *Blimp*-1 mutant embryos. We labeled the apical cell junctions in *Blimp-1* mutant embryos and found that the apical cell shape differed to that of *wt* cells (Figure 1, J–N). In *Blimp-1* mutants, the longest cell axis appeared to be perpendicular to the tube axis, while in the *wt* it was parallel (Figure 1, J–M). Most of the *Blimp-1* mutant cells had a reduced apical cell surface area when compared to wt cells, thereby suggesting a uniform organization throughout the tube (except for the fusion cells, which already had a distinct apical cell shape that did not seem to be affected by the loss of function of *Blimp-1*) (Figure 1K). To have a better idea of cell organization in *Blimp-1* mutant trachea, we traced tracheal cell surfaces and compared them to those of the *wt*. We observed altered cell shapes in the former. In this regard, the mutant trachea showed cells that were less elongated and more "square-shaped" than *wt* ones (Figure 1, L and M). In addition, when the apical cell surface areas were measured, we could conclude that apical cell surface area in Blimp-1 mutants was reduced to about half of wt apical cell surface area (Figure 1N).

Taken together, these observations reveal that Blimp-1 affects various stages of tube maturation, from chitin deposition to tube expansion, as well cellular morphology.

Blimp-1 modulates the timing of chitin deposition

In *wt* embryos, a matrix composed of chitin and proteins such as Gasp, accumulates in the tracheal lumen. This matrix plays a key role in the regulation of tube length and diameter expansion (Moussian *et al.* 2005, 2015; Tonning *et al.* 2005). Due to the striking tube size phenotype of *Blimp-1* mutants, and, because mutations in genes involved in chitin biogenesis and assembly result in irregular diametric expansion leading to locally constricted and dilated tubes, we examined the deposition of these markers from stage 12 (Figure 2). In the *wt*, early chitin deposition began at stage 13, when a chitinous filament started to be deposited inside the DT just prior to tube expansion (Moussian *et al.* 2015). In parallel, Gasp was detected from stage 13, but at this stage it was mainly cytoplasmic. None of these markers were detected at earlier stages. At stage 13, chitin began to be deposited in the lumen of all branches, starting from the DT (Moussian *et al.* 2015), and a mature pattern was achieved at stage 17, when taenidial ridges are fully formed (Tiklová *et al.* 2013; Öztürk-Çolak *et al.* 2016). *Blimp-1* mutant embryos showed chitin deposition as early as stage 12 (Figure 2, B and C). The pattern of chitin deposition in mutants at stage 13 was similar to that of the *wt* (Figure 2, D and F). However, at later stages, the trachea of *Blimp*-1 mutants showed lower levels of chitin than the *wt* (Figure 2G) (Öztürk-Çolak *et al.* 2016). Gasp levels were lower in *Blimp-1* mutants throughout embryogenesis, especially in the DT during later stages (Figure 2K), a pattern resembling that of embryos mutant for genes involved in chitin synthesis and organization (Araújo *et al.* 2005). We have previously shown that when we overexpressed *Blimp-1* in the posterior part of the embryo using

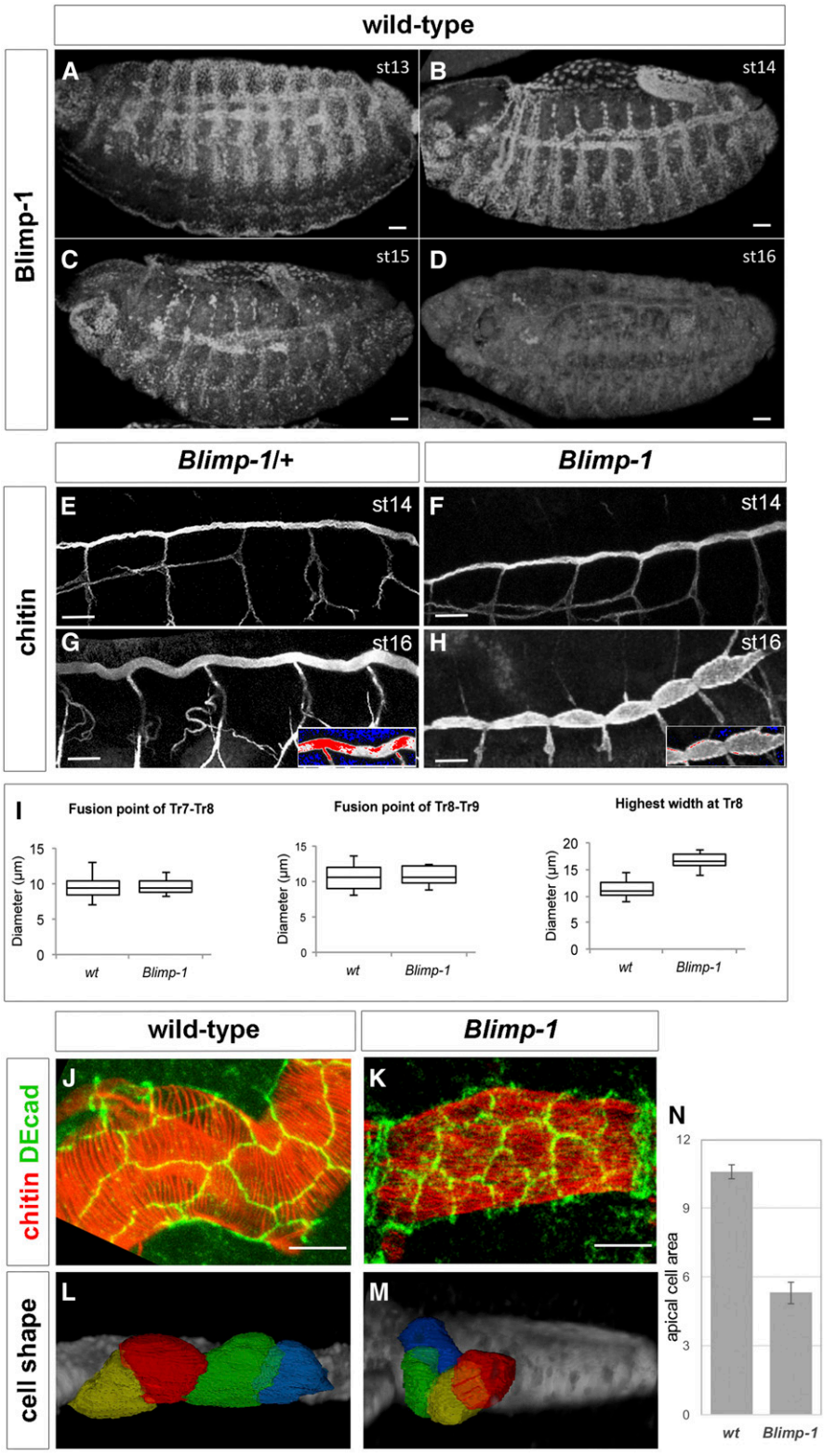

Figure 1 Blimp-1 is required for tracheal tube maturation. (A–D) Wild-type embryos stained for Blimp-1 protein with an anti-Blimp-1 antibody and showing Blimp-1 localization in tracheal cells from stage 13 to stage 15. At stage 15, Blimp-1 starts to be downregulated from the dorsal trunk (DT) and protein is not detected in tracheal cells at stage 16. Bar, 20 µm. (E–H) At stage 14, *Blimp-1* tracheal DT is not distinguishable from the wild-type DT. Differences are observed at later stages of development, when *Blimp-1* embryos display DTs with tube expansions between DT fusion points (H). (G and H) insets show detail of DT under a HiLo LUT, where highest intensity levels are red and lowest are blue, so differences in chitin amounts can be observed. Bar, 10 µm. (I) Quantification of tube width at fusion points and at between fusion points. (J–M) *Blimp-1* DT tracheal cells have smaller apical domains than wild-type DT tracheal cells. Bar, 5 µm. (N) Quantification of apical cell surface area in wt and *Blimp-1* DTs (n = 15, P-value <0.001).

Abd-BGAL4 to create tracheal DTs with distinct cellular compositions (Förster *et al.* 2009), we could detect lower levels of chitin in the posterior domain expressing higher levels of *Blimp-1* (Öztürk-Çolak *et al.* 2016). To further analyze the influence of Blimp-1 in timely chitin deposition, we used the same experimental conditions and found that chitin was hardly detected in the posterior part of the trachea (Figure 2L) (Öztürk-Çolak *et al.* 2016). However, further examination with higher laser power and gain showed that indeed both the chitin filament and taenidia were present

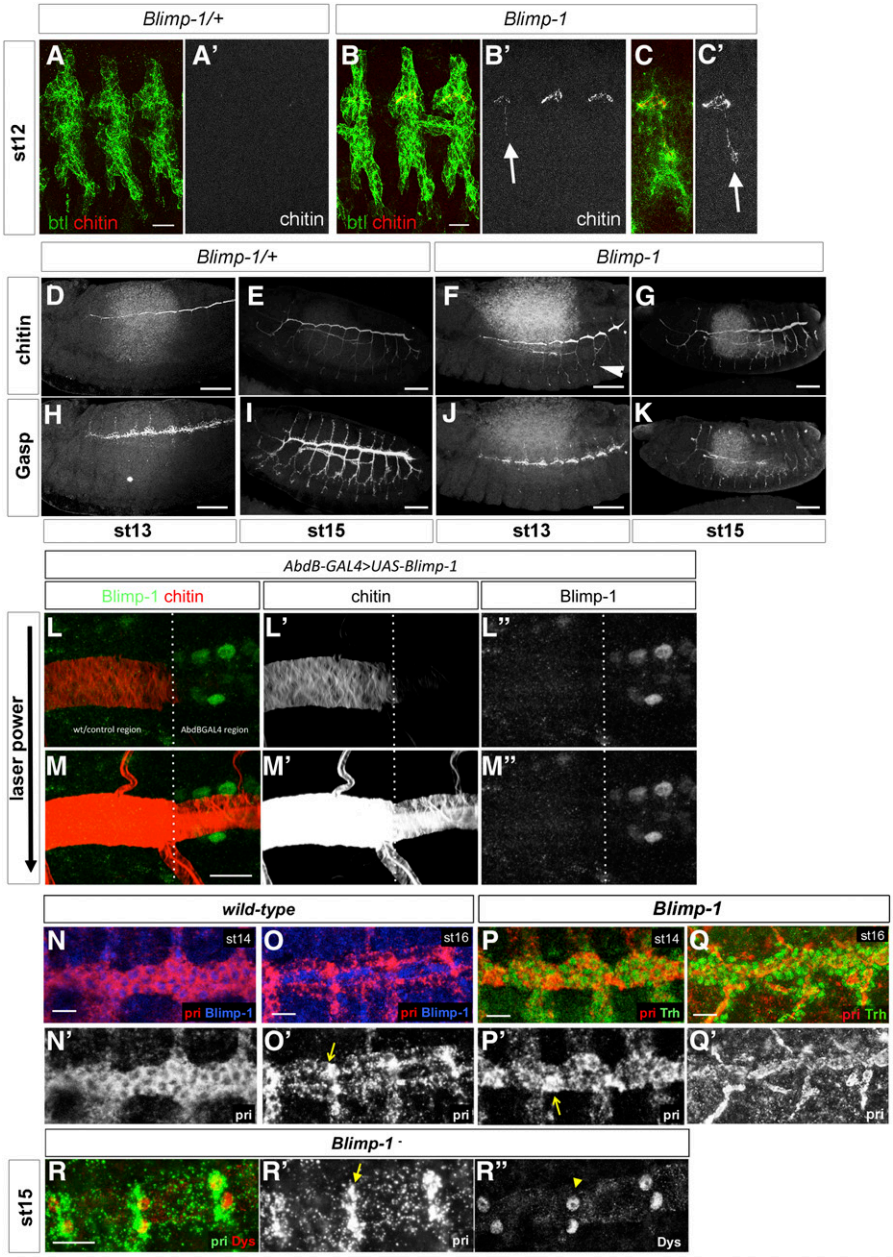

Figure 2 The timing of tube maturation is altered in *Blimp-1* mutants. (A–C) The deposition of chitin in *Blimp-1* embryos starts earlier than in the wild type and can be detected in the primordia of the DT and in some of the transverse connectives (LTs, arrows) from stage 12 (B, B′ and C, C′ versus A, A′). Btl positive cells are detected by a btl::moeGFP construct, stained with GFP. Bar, 5 μm. (D–K) Comparison of chitin and Gasp deposition in heterozygous (D, E, H, and I) *vs.* homozygous (F, G, J, and K) *Blimp-1* embryos. Gasp deposition is defective in *Blimp-1* embryos at stage 15, regardless of earlier chitin deposition. Bar, 40 μm. (L, L′, L′′ and M, M′, M′′) Detail of an early stage 17 DT at the border between cells expressing normal *Blimp-1* levels and higher Blimp-1 levels driven by AbdBGAL4. Overexpression of *Blimp-1* delays tube maturation, as reflected by lower chitin deposition. Bar, 10 μm. (N–P) Fluorescent *in situ* hybridization of *pri* (red) costained with either anti-Blimp-1 (blue) to label *Blimp-1*-expressing cells, or anti-Trh (green) to label tracheal cells, in wild-type stage 14 (N) and stage 16 (O) and *Blimp-1* mutant stage 14 (P) embryos. In wild-type embryos, at stage 14 *pri* is uniformly expressed throughout the tube (N′). Later, at stage 16, *pri* expression starts to gradually disappear except at fusion points (O′, arrow). In the *Blimp-1* mutant embryo this differential expression of *pri* is already present at stage 14. Note the lower levels of *pri* expression throughout the tube at stage 14 of the *Blimp-1* mutant embryo (P′), except at the fusion points (arrow). (Q,Q′) *pri* expression at stage 16 *Blimp-1* mutant embryos. Bar, 10 μm. (QR) *pri*-expressing cells in *Blimp-1* loss of function correspond to the fusion cells. Fluorescent *in situ* hybridization of pri (green) costained with anti-Dys (red) to label fusion cells in a *Blimp-1* mutant embryo at stage 15. The *pri* expression (arrow in R′) colocalizes with *dys* expression (arrowhead in R′′), indicating that the *pri*-expressing cells are fusion cells.

throughout the trachea, although they displayed much lower levels in the posterior metameres, resembling chitin levels at earlier stages of development (Figure 2M). *Blimp-1* overexpression lead to a tubular structure that regarding chitin composition and organization was apparently younger than the same tube with normal levels of Blimp-1 protein. Thus, Blimp-1 seems to regulate the timing of the beginning of chitin deposition by repressing target proteins. When Blimp-1 levels are high, chitin deposition is delayed, whereas, when they are low, chitin deposition begins earlier in the tracheal tubes.

The expression pattern of tarsal-less/polished rice is altered in Blimp-1 mutants

Mutants for *tarsal-less* (*tal*), also known as *polished rice* (*pri*), are affected in both F-actin and taenidia organization, and we analyzed them in parallel to *Blimp-1* mutants (Öztürk-Çolak *et al.* 2016). Like *Blimp-1*, the tracheal expression of *tal/pri* in wild-type embryos is regulated by ecdysone (Chanut-Delalande *et al.* 2014) (Figure S1) and started in tracheal cells at stage 12 (Figure S2). At early stages this expression was restricted to DT cells, but was later observed uniformly in all tracheal cells until stage 15 (Figure S2). From this stage, *tal/pri* expression gradually decreased in all DT cells, except fusion cells, and, at stage 16, coinciding with the time Blimp-1 disappears from tracheal cells, it became lower in almost all DT cells except in fusion cells (Figure 2O and Figure S2). *tal/pri* expression in *Blimp-1* mutants at stage 14 was not uniform in DT cells as in the *wt*. It was higher in fusion cells relative to the other DT cells (Figure 2P). To verify whether the cells with higher *tal/pri* expression in comparison to the

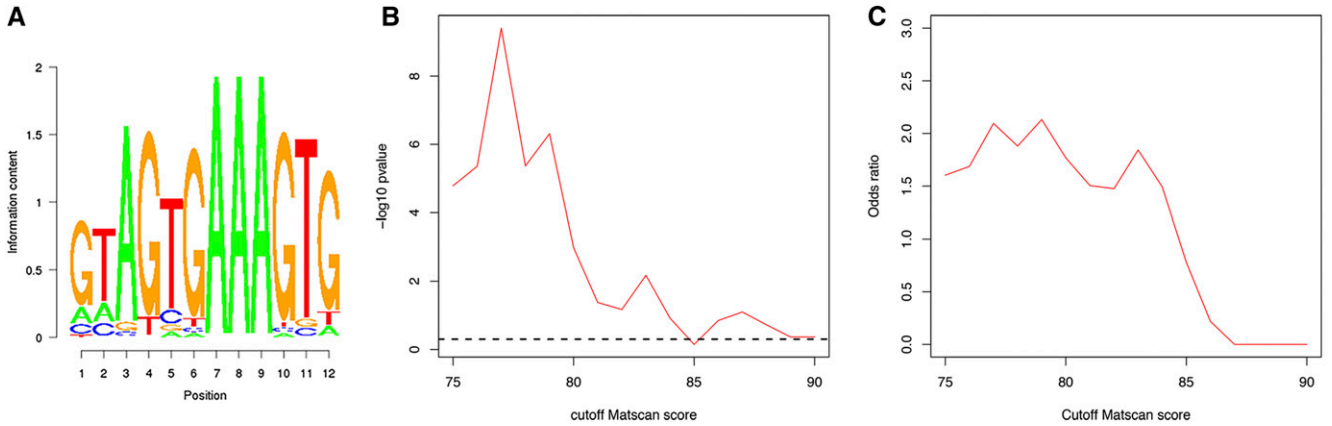

Figure 3 Blimp-1 position weight matrix. (A) Position weight matrix used in this study, which was taken from the reported binding sequences in Kuo and Calame (2004). (B and C) Enrichment analysis of known tracheal genes among genes predicted to be regulated by Blimp-1. *P*-values and ORs are shown for Fisher tests with varying Matscan scores for the definition of predicted binding sites. For values <85, ORs are relatively constant and >1.5 (associated *P*-values <0.05, dashed line) showing robustness against variations of the Matscan parameter.

other DT cells were indeed fusion cells, we double labeled the embryos with the fusion cell marker *dysfusion* (*dys*) (Jiang and Crews 2003). Higher levels of both *tal/pri* and *dys* were detected in the same cells, thereby confirming that these are indeed fusion cells (Figure 2Q). These results indicate that *tal/pri* expression at stage 14 *Blimp-1* embryos resembles expression of *tal/pri* in stage 16 *wt* embryos, suggesting that *Blimp-1* regulates the timing of the onset of *tal/pri* differential expression, from embryonic stage 16. We hypothesize that Blimp-1 might be involved in the differential regulation of *tal/pri* expression in tracheal cells. When Blimp-1 levels are low, *tal/pri* expression levels go down in DT, and are maintained at high levels only in fusion cells. We speculate that Blimp-1 could play a role in repressing *tal/pri* expression at high levels in fusion cells and, from stage 16, when Blimp-1 is no longer present in tracheal cells, this repression would no longer be exerted, leading to higher levels of expression in fusion cells.

Blimp-1 regulates a variety of genes involved in tube maturation

To further study the influence of *Blimp-1* in tracheal development, we searched *in silico* for Blimp-1 binding sites in the promoter regions of all *D. melanogaster* genes using the Matscan software (Blanco *et al.* 2006) and the reported position weight matrix corresponding to Blimp-1 (Kuo and Calame 2004). We found 3949 genes (6332 different isoforms) with at least one putative binding site (binding score >75% of maximum value) within 2000 bases of their annotated TSSs. We prioritized candidate positions on the basis of binding score and evolutionary conservation from the UCSC *Drosophila*-related species track (Fujita *et al.* 2011) (Table S1). In particular, we found that Blimp-1 can potentially regulate its own transcription, and also the transcription of a variety of genes involved in tracheal tube development. We asked whether Blimp-1 regulation of tracheal genes was enriched in relation to all genes in the fly genome. The transcription factor Trachealess (Trh) is among the first genes to be expressed in the cells that will form the trachea. In the absence of Trh, tracheal cells fail to invaginate to form tubes and remain at the embryo surface (Isaac and Andrew 1996; Wilk *et al.* 1996). It has been shown that expression of nearly every tracheal gene requires *trh* (Chung *et al.* 2011). Thus, we wondered how many genes regulated by Blimp-1 were also downstream of Trh, and, therefore, *bona fide* tracheal genes. To test this, we combined published tracheal gene sets (Chung *et al.* 2011; Hammonds *et al.* 2013) and checked for enrichment among the genes with predicted Blimp-1 binding sites. We found that for a conservation threshold of 2 and Matscan scores >75%, tracheal genes are significantly enriched [Fisher-test odds ratio (OR) = 1.60, *P*-value <0.001]. In order to show robustness against the choice of Matscan score threshold, we repeated the Fisher test for values ranging from 75 to 90%. We found that the OR was kept relatively constant until 84%, dropping to nonsignificant values for the remaining thresholds (Figure 3, B and C and Table S3).

We then selected a shorter list of genes reported to be involved in tube maturation stages (Table 1). Clearly, this is not an exhaustive list as it includes only the genes detected using these restrictive parameters. Thus, for example, this analysis did not allow us to detect any Blimp-1 binding sites in the *tal/pri* region. However, due to the changes in *tal/pri* expression in *Blimp-1* mutants, we further studied the *tal/pri* region under less restrictive conditions. We detected four binding sites with Matscan scores above the 72 percentile and conservation scores of 1.

Blimp-1 regulates the levels of Exp, Reb, aPKC, Knk, and Btk29A

In order to further analyze the relationship between *Blimp-1* and tracheal maturation, we compared the levels of five key proteins, Exp, Reb, aPKC, Knk, and Btk29A, in tube maturation in the heterozygous and homozygous *Blimp-1* mutant

Table 1 Possible downstream targets of Blimp-1 known to be involved in tracheal tube maturation

Gene	Function	Reference
atypical Protein Kinase C (aPKC)	Member of the Par complex	Hosono *et al.* (2015)
bitesize (btsz)	Synaptotagmin-like protein	JayaNandanan *et al.* (2014)
Blimp-1	Transcription factor	Chavoshi *et al.* (2010)
Btk family kinase at 29A (Btk29A)	Nonreceptor tyrosine kinase	Tsikala *et al.* (2014)
expansion (*exp*)	Required for chitin deposition	Moussian *et al.* (2015)
gartenzwerg (garz)	Secretion	Chung *et al.* (2011)
grainy-head (grh)	Transcription factor	Hemphälä *et al.* (2003)
knickhopf (knk)	Chitin organization	Chung *et al.* (2011)
obstructor-A (obst-A)	Chitin-binding protein	Chung *et al.* (2011)
pebbled (peb)	Transcription factor	Wilk *et al.* (2000)
rebuf (reb)	Required for chitin deposition	Moussian *et al.* (2015)
shade (shd)	Ecdysone pathway enzyme	Chavoshi *et al.* (2010)
sinuous (sinu)	Septate junction component	Wu *et al.* (2004)
tramtrack (ttk)	Transcription factor	Araújo *et al.* (2007)

Matscan score within the upper 75 percentile (and conservation score >2).

embryos. Exp and Reb are atypical Smad-like proteins that regulate tube size in the tracheal system by promoting chitin deposition (Moussian *et al.* 2015). aPKC is a serine/threonine protein kinase required for apico-basal cell polarity and a member of the Par complex. It has been shown to be involved in the orientation of actin rings and taenidial ridges in larval stages of tube maturation (Hosono *et al.* 2015). Knk is a GPI anchored protein needed for chitin organization and the regulation of tracheal tube diameter (Moussian *et al.* 2006). Btk29A (also known as Tec29A) is the only member of the Tec family of kinases in *Drosophila*, and it is expressed in many developmental stages of the fly. In the tracheal system, Btk29A is involved in spiracular chamber invagination, as well as in tracheal cuticle patterning (Matusek *et al.* 2006; Tsikala *et al.* 2014). Mutants and overexpression conditions for each of these genes showed phenotypes that can be correlated to the *Blimp-1* tracheal maturation phenotypes. We therefore hypothesized that Blimp-1 acts as a transcriptional repressor of these genes during tube maturation (Matusek *et al.* 2006; Moussian *et al.* 2006, 2015; Hosono *et al.* 2015).

At early tube maturation stages, *Blimp-1* mutants displayed higher levels of Exp, aPKC, Knk, and Btk29A than same-stage *wt* embryos (Figure 4), thereby suggesting that Blimp-1 represses the expression of these proteins, as hypothesized. Of the four proteins studied, Btk29A levels showed a more pronounced difference between heterozygous and homozygous *Blimp-1* mutant embryos. Btk29A levels at stage 14 were hardly detectable in the tracheal system of *wt* embryos (Figure 4G') (Tsikala *et al.* 2014), whereas, in mutant tracheal cells, they were detected at much higher levels (Figure 4H'). Taken together with our previous *in silico* approach, our findings suggest that Blimp-1 directly regulates the levels of these five proteins in tracheal cells during tube maturation, working as a repressor during early tracheal developmental stages.

During lumen maturation, chitin deposition requires the activity of Krotzkopf verkehrt (Kkv) together with Exp and Reb (Moussian *et al.* 2015). However, we could not find any evidence that Blimp-1 regulates *kkv* expression. Due to the earlier chitin deposition observed in *Blimp-1* mutant embryos (Figure 2), we wondered if Reb expression was also detected earlier, consequently leading to earlier chitin deposition. Indeed, we observed that in Blimp-1 homozygous embryos, Reb expression was already detected at stage 12, in contrast to wild-type and Blimp-1 heterozygous embryos, where it starts being detected at stage 13 (Figure 4, I–L) (Moussian *et al.* 2015). Thus, the earlier chitin deposition detected in *Blimp-1* embryos may be triggered by this earlier expression of Reb together with the higher levels of Exp in tracheal cells.

Btk29A works downstream of Blimp-1 to regulate luminal aECM organization

What is the role of Btk29A in tube maturation downstream of Blimp-1? At late embryonic stages, a strong *Btk29A* mutant allele displays disorganized apical F-actin bundles and taenidial ridges (Matusek *et al.* 2006; Öztürk-Çolak *et al.* 2016), with heterogeneous patterns of F-actin bundling in the same trachea, showing stretches of perpendicular bundles followed by stretches of parallel bundles (Öztürk-Çolak *et al.* 2016). In addition, overexpression of full-length *Btk29*A in all tracheal cells gave rise to an expansion phenotype similar to *Blimp-1* mutants at stage 16 (Figure 5C, cf. Figure 1H). Thus, and due to our hypothesis of *Blimp*-1 being a repressor of *Btk29*A expression, we examined whether derepression of Btk29A might partially account for the *Blimp-1* mutant phenotype. To do so, we used $Btk29A^{K00206}$, a hypomorphic allele in which low mRNA levels are still detected in the embryonic tracheal system (Tsikala *et al.* 2014). In this hypomorphic allele, there were no apparent differences in chitin deposition between heterozygous and homozygous *Btk29A* mutant embryos at stage 16 (Figure 5, A and B). At late stage 17, *Btk29*A ^{K00206} homozygous embryos showed mild DT phenotypes compared to heterozygous embryos, such as a very mild DT expansion phenotype (Figure 5, D and E). However, there were no detectable taenidial ridge orientation phenotypes in stage 17 $Btk29A^{K00206}$ mutants,

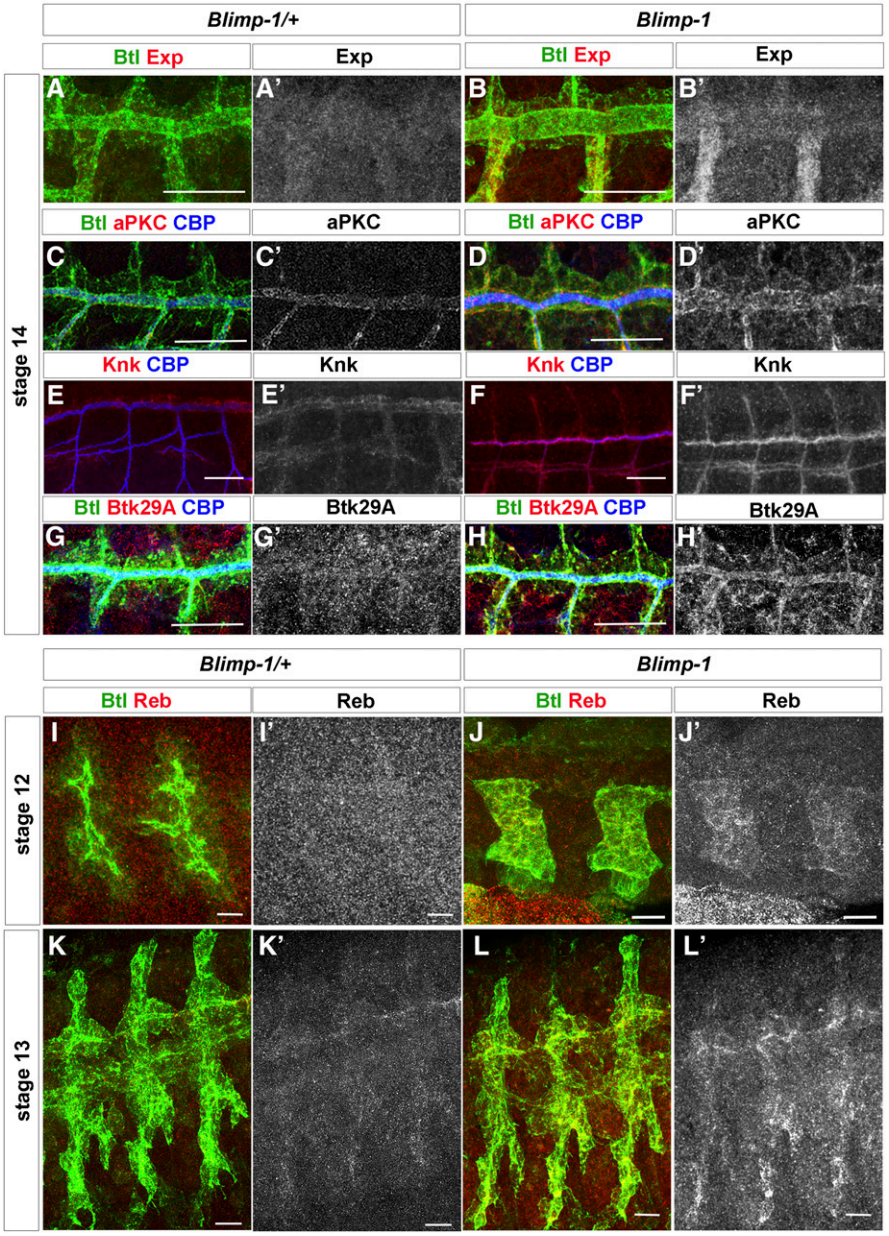

Figure 4 Blimp-1 regulates the expression of genes involved in tube maturation. (A, A′ and B, B′) Exp, (C, C′ and D, D′) aPKC, (E, E′ and F, F′) Knk and (G, G′ and H, H′) Btk29A levels are higher in *Blimp-1* mutants than in the *wild-type* at stage 14. Bar, 20 μm. (I–L) Reb expression starts earlier in *Blimp-1* mutant embryos; it is already detected in stage 12 mutants whereas it starts at stage 13 in heterozygous *Blimp-1* embryos (I, I′ and J, J′); heterozygous stage 12 embryos in (I) are older than mutant embryos in (J) reinforcing the earlier expression of Reb in *Blimp-1* embryos. (K, K′ and L, L′) Reb expression is higher in stage 13 *Blimp-1* mutant embryos. Bar, 10 μm.

which showed parallel taenidial ridges perpendicular to the tube length as in the wild-type (Figure 5, E and E'). We then combined the *Btk29A*^{K00206} mutation with *Blimp-1* and observed that the incomplete removal of embryonic *Btk29A* could partially rescue the taenidial ridge orientation phenotypes in most of the embryos examined (64%, n = 11). These double *Btk29A*^{K00206}; *Blimp-1* mutants showed heterogeneous patterns of taenidial ridge organization in the same trachea, showing stretches of perpendicular bundles followed by stretches of parallel ones (45% of embryos, Figure 5, G and H, arrow in G), as well as diagonal ridges (19% of embryos, Figure 5H, arrow). We also observed that *Btk29A*; *Blimp-1* double mutant DTs showed a milder tube expansion phenotype than *Blimp-1* mutants (Figure 5, F–H). Taken together, these results indicate that part of the *Blimp-1* phenotype can be attributed to excess *Btk29A*.

Discussion

Here, we found that *Blimp-1* regulates multiple tracheal targets, thus acting as a key gene in tracheal development (Figure 6A and Table 1). *Blimp-1* is an ecdysone response gene (Beckstead *et al.* 2005; Chavoshi *et al.* 2010) (Figure S1) and, therefore, a link between the hormonal signal and the timing of tracheal tube maturation in both embryos and larvae. We show that *Blimp-1* regulates the expression of many genes required for tube maturation. Interestingly, *in silico*, we detected four Blimp-1 binding sites in *Blimp-1* regulatory sequences using the parameters described, which suggests that Blimp-1 may regulate its own expression. This is in agreement with recent data showing that Blimp-1/PRDM1 is also able to regulate its own expression in mammals (Mitani *et al.* 2017). Self-regulation of expression is consistent with

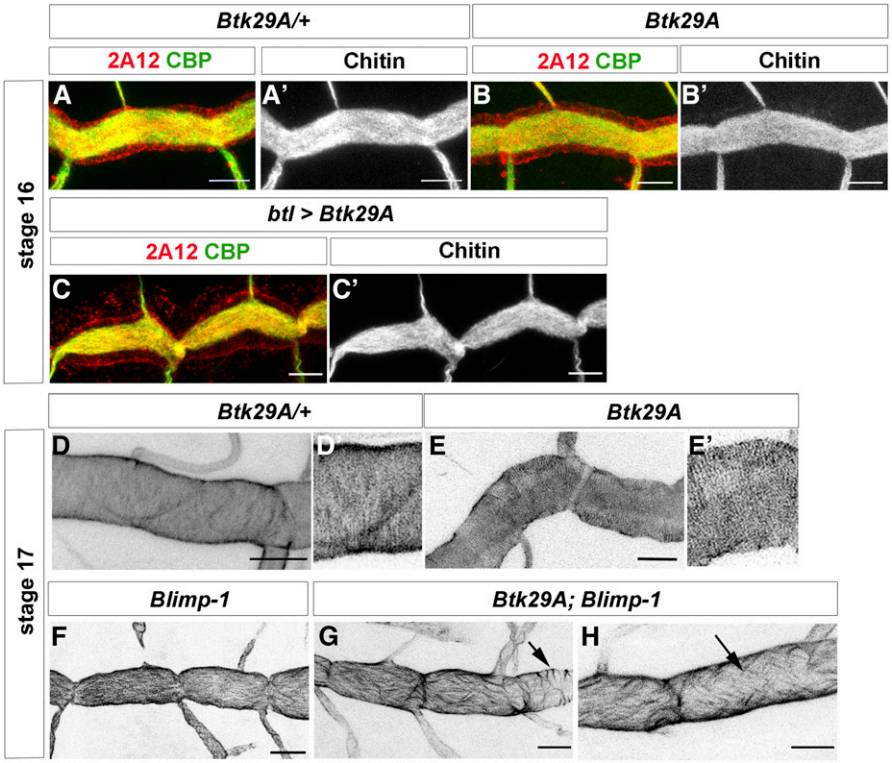

Figure 5 *Btk29A* partially rescues *Blimp-1* phenotypes. (A, A′ and B, B′) *Btk29A*^{K00206} embryos do not show any strong tube maturation phenotypes at late embryonic stages. (C, C′ and D, D′) *Btk29A* overexpression in tracheal cells induces tracheal phenotypes similar to *Blimp-1* mutant embryos. (D–H) At the end of embryogenesis, stage 17, taenidial ridges can be detected by staining with chitin binding probes (CBP) (D and D′); *Btk29A* ^{K00206} embryos display mild taenidial ridge phenotypes (E and E′); however, when in a *Blimp-1* mutant background, a *Btk29A* hypomorphic mutation such as the one present in the K00206 allele, partially rescues the *Blimp-1* expansion and taenidial ridge phenotypes (G and H). Bar, 5 μm in all panels.

the feedback loops in which Blimp-1/PRDM1 participates, and also with its role in regulating many developmental processes (Gong and Malek 2007; Bikoff *et al.* 2009). We also found Blimp-1 binding sites in the region of Tramtrack (Ttk), another transcription factor involved in many features of tube maturation (Araújo *et al.* 2007).

Furthermore, we observed that *Blimp-1* modulates the timing of the expression of *reb* and *exp*, two genes involved in the genetic program triggering timely chitin deposition (Moussian *et al.* 2015). Untimely chitin deposition was shown to disturb tube maturation, thereby demonstrating that this process has to be tightly regulated during tracheal development. Tracheal overexpression of *reb* leads to earlier chitin deposition in all branches from stage 13 and sometimes chitin appearance at stage 12 (Moussian *et al.* 2015; and M. Llimargas, personal communication). Accordingly, our results show that Reb is expressed earlier in *Blimp-1* embryos (Figure 4, J and L). This agrees with the early chitin deposition phenotypes observed in

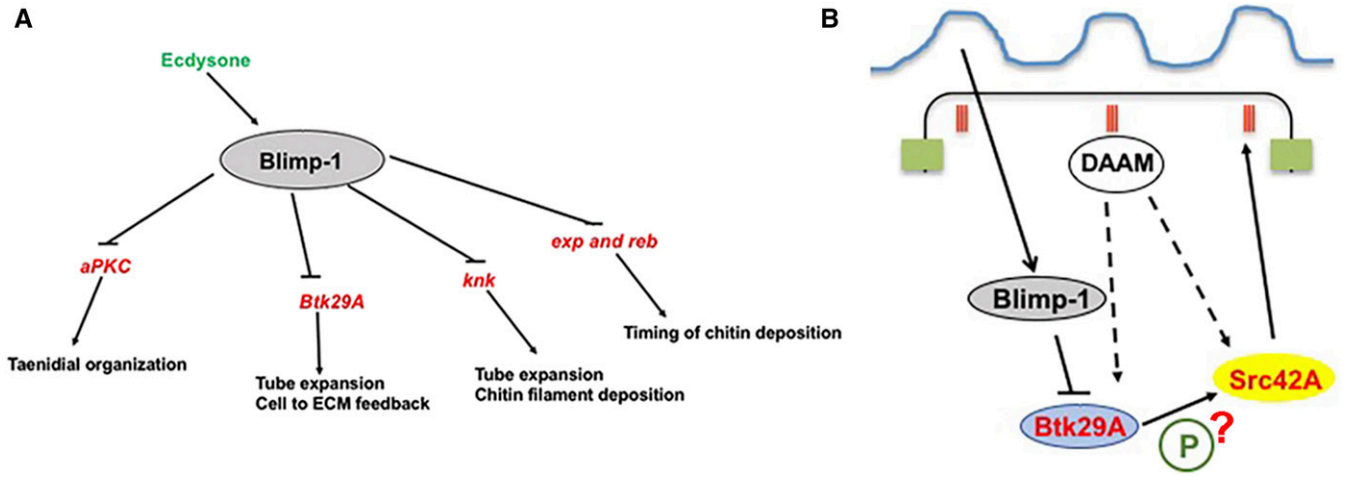

Figure 6 A model for the involvement of *Blimp-1* in tracheal tube maturation timing. (A) Under the influence of the insect hormone ecdysone, Blimp-1 regulates tracheal tube maturation timing by inhibiting the expression of the key genes for tube maturation, among them *aPKC*, *Btk29A*, *knk*, *exp*, and *reb*. Some of these targets are known to be activated by other transcription factors, like, for example, Ttk in the case of Exp, Spalt (Sal) in the case of Reb, and Trh in the case of Knk (Chung *et al.* 2011; Moussian *et al.* 2015). (B) Blimp-1 affects taenidial ridge formation by acting as a transcriptional repressor of Btk29A, which is an important molecule for Src42A phosphorylation. Phosphorylated Src42A and the formin DAAM regulate the actin cytoskeleton inside the cells, hence giving rise to taenidial ridges at the extracellular matrix.

Blimp-1 mutants (Figure 2, B and C). Furthermore, *Blimp-1* also modulated *knk* expression during tube maturation stages. Knk is involved in directing chitin assembly in the trachea (Moussian *et al.* 2006) and correct amounts of Knk at specific times during metamorphosis are important for correct wing cuticle differentiation and function (Li *et al.* 2017). Taken together, these *in silico* and *in vivo* results indicate that Blimp-1 is a transcription factor that acts downstream of ecdysone, and that it is involved in the correct timing of chitin synthesis and deposition during embryonic development.

We also found Blimp-1 binding sites in the aPKC coding region. aPKC is involved in the junction anisotropies that orient both actin rings and taenidial ridges in the lumen of tracheal tubes (Hosono *et al.* 2015). In *Blimp-1* mutants, both actin rings and taenidial ridges are either undetectable or misoriented (Öztürk-Çolak *et al.* 2016)—observations that are consistent with changes in junction anisotropy.

We previously showed that Blimp-1 regulates chitin deposition levels and architecture, and that, subsequently, the chitin aECM feeds back on the cellular architecture by stabilizing F-actin bundling and cell shape via the modulation of Src42A phosphorylation levels (Öztürk-Çolak *et al.* 2016). However, in this report, we provided no link between the chitinous aECM and Src42A. *Btk29A* mutant larvae have an aECM phenotype, which may be the result of their actin bundle phenotype (Matusek *et al.* 2006; Öztürk-Çolak *et al.* 2016). Here, we found that *Btk29A* removal can partially rescue the *Blimp-1* taenidial orientation and expansion phenotype. In view of these results, we propose that the contribution of Btk29A can be added to the feedback model for the generation of supracellular taenidia put forward in Öztürk-Çolak *et al.* (2016). We now add to our previous model by hypothesizing that Blimp-1 acts as a link between the aECM and cells by regulating the levels of Btk29A (Figure 6B). Btk29A and Src42A, together with the formin DAAM, have been shown to regulate the actin cytoskeleton (Matusek *et al.* 2006). In agreement with our results, we speculate that Btk29A might phosphorylate Src42A, and that this phosphorylation event could be modulated by Blimp-1 and DAAM.

To conclude, our results indicate that Blimp-1 is a key player in the regulation of tracheal tube maturation, and, consequently, in the feedback mechanism involved in the generation of supracellular taenidia.

Acknowledgments

We thank M. Llimargas, E. Sanchez-Herrero, S. Roy, H. Ueda, and the Bloomington Stock Center for flies and reagents. Thanks also go to the Institut de Recerca Biomedica de Barcelona (IRB Barcelona) Biostatistics and Bioinformatics Unit. We acknowledge L. Bardia, A. Lladó, and J. Colombelli from the IRB Barcelona Advanced Digital Microscopy Facility for help and advice with confocal microscopy and software, and E. Fuentes and N. Martin for technical assistance. S.J.A. was a Ramon y Cajal Researcher (RYC-2007-00417); A.O. was the recipient of an IRB-La Caixa fellowship. This work was supported by grants from the Generalitat de Catalunya and the Spanish Ministerio de Ciencia e Innovación (BFU2009-07629).

Literature Cited

Agawa, Y., M. Sarhan, Y. Kageyama, K. Akagi, M. Takai *et al.*, 2007 Drosophila Blimp-1 is a transient transcriptional repressor that controls timing of the ecdysone-induced developmental pathway. Mol. Cell. Biol. 27: 8739–8747. https://doi.org/10.1128/MCB.01304-07

Akagi, K., M. Sarhan, A.-R. S. Sultan, H. Nishida, A. Koie *et al.*, 2016 A biological timer in the fat body comprising Blimp-1, βFtz-f1 and Shade regulates pupation timing in Drosophila melanogaster. Development 143: 2410–2416. https://doi.org/10.1242/dev.133595

Araújo, S. J., H. Aslam, G. Tear, and J. Casanova, 2005 Mummy/cystic encodes an enzyme required for chitin and glycan synthesis, involved in trachea, embryonic cuticle and CNS development–analysis of its role in Drosophila tracheal morphogenesis. Dev. Biol. 288: 179–193. https://doi.org/10.1016/j.ydbio.2005.09.031

Araújo, S. J., C. Cela, and M. Llimargas, 2007 Tramtrack regulates different morphogenetic events during Drosophila tracheal development. Development 134: 3665–3676. https://doi.org/10.1242/dev.007328

Beckstead, R. B., G. Lam, and C. S. Thummel, 2005 The genomic response to 20-hydroxyecdysone at the onset of Drosophila metamorphosis. Genome Biol. 6: R99. https://doi.org/10.1186/gb-2005-6-12-r99

Bikoff, E. K., M. A. Morgan, and E. J. Robertson, 2009 An expanding job description for Blimp-1/PRDM1. Curr. Opin. Genet. Dev. 19: 379–385. https://doi.org/10.1016/j.gde.2009.05.005

Blanco, E., X. Messeguer, T. F. Smith, and R. Guigo, 2006 Transcription factor map alignment of promoter regions. PLOS Comput. Biol. 2: e49. https://doi.org/10.1371/journal.pcbi.0020049

Campos-Ortega, A. J., and V. Hartenstein, 1985 The Embryonic Development of Drosophila Melanogaster, pp. 10–84. Springer-Verlag, New York. https://doi.org/10.1007/978-3-662-02454-6

Chanut-Delalande, H., Y. Hashimoto, A. Pelissier-Monier, R. Spokony, A. Dib *et al.*, 2014 Pri peptides are mediators of ecdysone for the temporal control of development. Nat. Cell Biol. 16: 1035–1044. https://doi.org/10.1038/ncb3052

Chavoshi, T. M., B. Moussian, and A. Uv, 2010 Tissue-autonomous EcR functions are required for concurrent organ morphogenesis in the Drosophila embryo. Mech. Dev. 127: 308–319. https://doi.org/10.1016/j.mod.2010.01.003

Chung, S., C. Chavez, and D. J. Andrew, 2011 Trachealess (Trh) regulates all tracheal genes during Drosophila embryogenesis. Dev. Biol. 360: 160–172. https://doi.org/10.1016/j.ydbio.2011.09.014

Cunningham, F., M. R. Amode, D. Barrell, K. Beal, K. Billis *et al.*, 2015 Ensembl 2015. Nucleic Acids Res. 43: D662–D669. https://doi.org/10.1093/nar/gku1010

Fog, C. K., G. G. Galli, and A. H. Lund, 2012 PRDM proteins: important players in differentiation and disease. BioEssays 34: 50–60. https://doi.org/10.1002/bies.201100107

Förster, D., K. Armbruster, and S. Luschnig, 2009 Sec24-dependent secretion drives cell-autonomous expansion of tracheal tubes in Drosophila. Curr. Biol. 20: 62–68. https://doi.org/10.1016/j.cub.2009.11.062

Fujita, P. A., B. Rhead, A. S. Zweig, A. S. Hinrichs, D. Karolchik *et al.*, 2011 The UCSC genome browser database: update 2011. Nucleic Acids Res. 39: D876–D882. https://doi.org/10.1093/nar/gkq963

Gong, D., and T. R. Malek, 2007 Cytokine-dependent Blimp-1 expression in activated T cells inhibits IL-2 production.

J. Immunol. 178: 242–252. https://doi.org/10.4049/jimmunol.178.1.242

Hammonds, A. S., C. A. Bristow, W. W. Fisher, R. Weiszmann, S. Wu *et al.*, 2013 Spatial expression of transcription factors in Drosophila embryonic organ development. Genome Biol. 14: R140. https://doi.org/10.1186/gb-2013-14-12-r140

Hemphälä, J., A. Uv, R. Cantera, S. Bray, and C. Samakovlis, 2003 Grainy head controls apical membrane growth and tube elongation in response to Branchless/FGF signalling. Development 130: 249–258. https://doi.org/10.1242/dev.00218

Hohenauer, T., and A. W. Moore, 2012 The Prdm family: expanding roles in stem cells and development. Development 139: 2267–2282. https://doi.org/10.1242/dev.070110

Hosono, C., R. Matsuda, B. Adryan, and C. Samakovlis, 2015 Transient junction anisotropies orient annular cell polarization in the Drosophila airway tubes. Nat. Cell Biol. 17: 1569–1576. https://doi.org/10.1038/ncb3267

Huang, S., 1994 Blimp-1 is the murine homolog of the human transcriptional repressor PRDI-BF1. Cell 78: 9. https://doi.org/10.1016/0092-8674(94)90565-7

Isaac, D. D., and D. J. Andrew, 1996 Tubulogenesis in Drosophila: a requirement for the trachealess gene product. Genes Dev. 10: 103–117. https://doi.org/10.1101/gad.10.1.103

JayaNandanan, N., R. Mathew, and M. Leptin, 2014 Guidance of subcellular tubulogenesis by actin under the control of a synaptotagmin-like protein and Moesin. Nat. Commun. 5: 3036. https://doi.org/10.1038/ncomms4036

Jiang, L., and S. T. Crews, 2003 The Drosophila dysfusion basic helix-loop-helix (bHLH)-PAS gene controls tracheal fusion and levels of the trachealess bHLH-PAS protein. Mol. Cell. Biol. 23: 5625–5637. https://doi.org/10.1128/MCB.23.16.5625-5637.2003

Keller, A. D., and T. Maniatis, 1991 Identification and characterization of a novel repressor of beta-interferon gene expression. Genes Dev. 5: 868–879. https://doi.org/10.1101/gad.5.5.868

Kuo, T. C., and K. L. Calame, 2004 B lymphocyte-induced maturation protein (Blimp)-1, IFN regulatory factor (IRF)-1, and IRF-2 can bind to the same regulatory sites. J. Immunol. 173: 5556–5563. https://doi.org/10.4049/jimmunol.173.9.5556

Li, K., X. Zhang, Y. Zuo, W. Liu, J. Zhang *et al.*, 2017 Timed Knickkopf function is essential for wing cuticle formation in Drosophila melanogaster. Insect Biochem. Mol. Biol. 89: 1–10. https://doi.org/10.1016/j.ibmb.2017.08.003

Matusek, T., A. Djiane, F. Jankovics, D. Brunner, M. Mlodzik *et al.*, 2006 The Drosophila formin DAAM regulates the tracheal cuticle pattern through organizing the actin cytoskeleton. Development 133: 957–966. https://doi.org/10.1242/dev.02266

Mitani, T., Y. Yabuta, H. Ohta, T. Nakamura, C. Yamashiro *et al.*, 2017 Principles for the regulation of multiple developmental pathways by a versatile transcriptional factor, BLIMP1. Nucleic Acids Res. 45: 12152–12169. https://doi.org/10.1093/nar/gkx798

Moussian, B., H. Schwarz, S. Bartoszewski, and C. Nusslein-Volhard, 2005 Involvement of chitin in exoskeleton morphogenesis in Drosophila melanogaster. J. Morphol. 264: 117–130. https://doi.org/10.1002/jmor.10324

Moussian, B., E. Tång, A. Tonning, S. Helms, H. Schwarz *et al.*, 2006 Drosophila Knickkopf and Retroactive are needed for epithelial tube growth and cuticle differentiation through their specific requirement for chitin filament organization. Development 133: 163–171. https://doi.org/10.1242/dev.02177

Moussian, B., A. Letizia, G. Martínez-Corrales, B. Rotstein, A. Casali *et al.*, 2015 Deciphering the genetic programme triggering timely and spatially-regulated chitin deposition. PLoS Genet. 11: e1004939 (erratum: PLoS Genet. 11: e1005054). https://doi.org/10.1371/journal.pgen.1004939

Ng, T., F. Yu, and S. Roy, 2006 A homologue of the vertebrate SET domain and zinc finger protein Blimp-1 regulates terminal differentiation of the tracheal system in the Drosophila embryo. Dev. Genes Evol. 216: 243–252. https://doi.org/10.1007/s00427-005-0044-5

Öztürk-Çolak, A., B. Moussian, S. Araujo, and J. Casanova, 2016 A feedback mechanism converts individual cell features into a supracellular ECM structure in Drosophila trachea. eLife 5: e09373. https://doi.org/10.7554/eLife.09373

Schindelin, J., I. Arganda-Carreras, E. Frise, V. Kaynig, M. Longair *et al.*, 2012 Fiji: an open-source platform for biological-image analysis. Nat. Methods 9: 676–682. https://doi.org/10.1038/nmeth.2019

Smedley, D., S. Haider, S. Durinck, L. Pandini, P. Provero *et al.*, 2015 The BioMart community portal: an innovative alternative to large, centralized data repositories. Nucleic Acids Res. 43: W589–W598. https://doi.org/10.1093/nar/gkv350

Tiklová, K., V. Tsarouhas, and C. Samakovlis, 2013 Control of airway tube diameter and integrity by secreted chitin-binding proteins in Drosophila. PLoS One 8: e67415. https://doi.org/10.1371/journal.pone.0067415

Tonning, A., J. Hemphälä, E. Tång, U. Nannmark, C. Samakovlis *et al.*, 2005 A transient luminal chitinous matrix is required to model epithelial tube diameter in the Drosophila trachea. Dev. Cell 9: 423–430. https://doi.org/10.1016/j.devcel.2005.07.012

Tsikala, G., D. Karagogeos, and M. Strigini, 2014 Btk-dependent epithelial cell rearrangements contribute to the invagination of nearby tubular structures in the posterior spiracles of Drosophila. Dev. Biol. 396: 42–56. https://doi.org/10.1016/j.ydbio.2014.09.019

Turner, C. A., D. H. Mack, and M. M. Davis, 1994 Blimp-1, a novel zinc finger-containing protein that can drive the maturation of B lymphocytes into immunoglobulin-secreting cells. Cell 77: 297–306. https://doi.org/10.1016/0092-8674(94)90321-2

Wilk, R., I. Weizman, and B. Z. Shilo, 1996 Trachealess encodes a bHLH-PAS protein that is an inducer of tracheal cell fates in Drosophila. Genes Dev. 10: 93–102. https://doi.org/10.1101/gad.10.1.93

Wilk, R., B. H. Reed, U. Tepass, and H. D. Lipshitz, 2000 The hindsight gene is required for epithelial maintenance and differentiation of the tracheal system in Drosophila. Dev. Biol. 219: 183–196. https://doi.org/10.1006/dbio.2000.9619

Wu, V. M., J. Schulte, A. Hirschi, U. Tepass, and G. J. Beitel, 2004 Sinuous is a Drosophila claudin required for septate junction organization and epithelial tube size control. J. Cell Biol. 164: 313–323. https://doi.org/10.1083/jcb.200309134

Communicating editor: N. Perrimon